Quantitative Proteomics Reveals Regulation of Dynamic Components within TATA-binding Protein (TBP) Transcription Complexes*[S]

Florence Mousson‡§¶, Annemieke Kolkman§¶‖**, W. W. M. Pim Pijnappel‡ ‡‡, H. Th. Marc Timmers‡ ‡‡§§, and Albert J. R. Heck‖‡‡¶¶

Affinity purification in combination with isotope labeling of proteins has proven to be a powerful method to discriminate specific from nonspecific interactors. However, in the standard SILAC (stable isotope labeling by amino acids in cell culture) approach dynamic components may easily be assigned as nonspecific. We compared two affinity purification protocols, which in combination revealed information on the dynamics of protein complexes. We focused on the central component in eukaryotic transcription, the human TATA-binding protein, which is involved in different complexes. All known TATA-binding protein-associated factors (TAFs) were detected as specific interactors. Interestingly one of them, BTAF1, exchanged significantly in cell extracts during the affinity purification. The other TAFs did not display this behavior. Cell cycle synchronization showed that BTAF1 exchange was regulated during mitosis. The combination of the two affinity purification protocols allows a quantitative approach to identify transient components in any protein complex. ***Molecular & Cellular Proteomics 7:845–852, 2008.***

The development of quantitative mass spectrometry has had a major impact in proteomics allowing quantification of protein expression levels under different conditions (1–3). Among the applications of quantitative mass spectrometry the accurate determination of specificity of protein-protein interactions is crucial to the understanding of multisubunit protein assemblies. To discriminate between specific and nonspecific interacting proteins within complexes, most widely used methods in quantitative proteomics are stable isotope labeling approaches such as SILAC,[1] ICAT, and isotopic differentiation of interactions as random or targeted (I-DIRT) (3–9). In the most common approach stable isotope-labeled amino acids are used in cell cultures (SILAC) in combination with affinity purification (3). In such experiments, two cell populations differing by the presence of a tagged protein are grown in identical culture media with the exception that the first medium contains a "light," *e.g.* naturally abundant isotope of a selected amino acid, whereas the second medium contains a "heavy," *e.g.* stable isotope version of this amino acid. The labeled amino acid is efficiently incorporated during protein synthesis in the cell. This leads to a difference in mass for chemically identical peptides that can be detected by mass spectrometry. Two populations of cells can be combined directly after harvesting, and subsequent purification will have the same effect on the heavy and light forms of the proteins. The relative abundance of proteins ("SILAC ratio") is derived by comparison of the integrated mass spectrometry peak areas of the labeled and unlabeled forms of a peptide. Incorporation of heavy forms of arginine and lysine offers the advantage that most tryptic peptides can be used for quantification.

The relevance of multisubunit protein assemblies in cellular regulation pathways is well recognized (10), but progress in determining pathways of assembly and disassembly of complexes and regulation of (individual) subunit exchange has been hampered by a lack of generic methods. The importance of developing such methods is stressed by observations that a single protein can reside simultaneously in multiple protein complexes of distinct functions. The TATA-binding protein (TBP) is an example of a protein involved in different functions (11). Transcription initiation by RNA polymerase (pol) II requires the binding of TBP to core promoter DNA that triggers the formation of the preinitiation complex by assembly of pol II and basal transcription factors. TBP does not exist as a monomeric protein in human cell extracts (12), but it resides in at least four distinct protein complexes in eukaryotic cells. First TBP is incorporated with 13–14 TBP-associated factors (TAFs) into the TFIID complex involved in pol II transcription (13). Next in pol I transcription, TBP is part of the SL1 complex consisting of four other subunits: TAF_I110, TAF_I63, TAF_I48, and TAF_I41 (14). The pol III system uses the TFIIIB complex consisting of TBP, Brf1, and Bdp1 proteins (15). Finally a major proportion of cellular TBP resides in the B-TFIID com-

From the ‡Department of Physiological Chemistry, University Medical Centre Utrecht, Universiteitsweg 100, 3584 CG Utrecht, The Netherlands and ‖Department of Biomolecular Mass Spectrometry, Bijvoet Center for Biomolecular Research and Utrecht Institute for Pharmaceutical Sciences, Utrecht University, Sorbonnelaan 16, 3584 CA Utrecht, The Netherlands

Received, July 5, 2007, and in revised form, December 17, 2007

Published, MCP Papers in Press, December 17, 2007, DOI 10.1074/mcp.M700306-MCP200

[1] The abbreviations used are: SILAC, stable isotope labeling by amino acids in cell culture; TBP, TATA-binding protein; TAF, TBP-associated factor; pol, RNA polymerase; TF, transcription factor; HA, hemagglutinin; 1D, one-dimensional.

© 2008 by The American Society for Biochemistry and Molecular Biology, Inc.
This paper is available on line at http://www.mcponline.org

Downloaded from http://www.mcponline.org/ by guest on October 20, 2019

plex (12). B-TFIID contains only another subunit, BTAF1 (named Mot1p in yeast cells), which belongs to the family of SNF2-like ATPases (16, 17) and has emerged as an essential element in the regulation of TBP recruitment and activity on the promoter (16).

TBP is essential for all three nuclear RNA polymerase systems, suggesting that regulation of the composition and dynamics of TBP complexes should be a fine tuned process. Illustrations of variations in the composition of TBP complexes are multiple. As an example, study of *taf4*$^{-/-}$ mouse embryonic fibroblasts revealed that TAF4 and its isoform TAF4b display distinct target gene specificities and that competition between the two proteins regulates expression of genes controlling cell proliferation (18). Expression of an isoform of TAF6 (TAF6δ) is specifically induced in apoptotic cells and correlates with TFIID complexes lacking TAF9 (19). TAF7 has been reported to be released from TFIID upon initiation of transcription (20). In addition, it has been shown that the repression of all nuclear transcription during mitosis (21) leads to changes in localization and composition of TBP complexes. Immunocytochemistry experiments indicated that the majority of TFIID is released from chromatin during mitosis (22). Mitotic phosphorylation of Bdp1 by CK2 results in dissociation from RNA pol III promoters (23), but Brf1, the other TFIIIB subunit, hyperphosphorylated during mitosis, remains associated with promoters along with TBP (24). Contrary to the accumulation of data on the variation in their composition, regulation of dynamics within TBP complexes is not well understood mainly because approaches to study subunit exchange within protein complexes are lacking.

Here we applied SILAC combined with affinity purification to investigate the specificity of protein complex interactions. Our results indicated that the standard SILAC/affinity purification may easily assign dynamic components as nonspecific. The comparison of two affinity purification protocols allowed us to investigate dynamics within TBP complexes. Among all the TAFs, BTAF1 was the only one to exchange during affinity purification, and this behavior was inhibited during mitosis. The combination of two affinity purification protocols provides a generic tool to identify in a quantitative manner transient components in any protein complex.

EXPERIMENTAL PROCEDURES

Materials and Reagents—Labeled L-arginine ([^{13}C,^{15}N]Arg) and L-lysine ([^{13}C,^{15}N]Lys) were from Sigma Isotec. Modified Eagle's medium deficient in arginine, lysine, and leucine was obtained from Cambrex. Non-labeled leucine, arginine, lysine and puromycin were obtained from Sigma. Dialyzed serum, L-glutamine, non-essential amino acids, penicillin/streptomycin, and trypsin were from Cambrex. FLAG peptide and M2 affinity resin were from Sigma, and HA peptide was from Sigma-Genosys. HA affinity resin was prepared by covalently binding 12CA5 HA antibody to Dynabeads-protein A (Dynal) using dimethyl pimelimidate dihydrochloride (Pierce) following the manufacturer's instructions.

Generation of Stable Cell Lines—Human TBP was introduced by GATEWAY cloning into retroviral destination plasmid derived from pBABE-puro carrying N-terminal HA and FLAG tags. HeLa S3 cell clones expressing HA/FLAG-tagged TBP were obtained by retroviral transduction and puromycin selection. Positive clones were identified by immunoblotting using 1F8 (25) and 3F10 (Roche Applied Science) antibodies directed against TBP and the HA tag, respectively.

Cell Culture Preparation and Cell Culture Conditions—Amino acid-deficient medium was supplemented with unlabeled leucine and either labeled or unlabeled arginine (498 μM) and lysine (405 μM). It was also supplemented with 10% dialyzed fetal bovine serum, glutamine, non-essential amino acids, and antibiotics. For SILAC, cells were grown for at least six cell divisions. When necessary cells were treated with 60 ng/ml nocodazole for 17 h. For cell cycle analysis, cells were stained with 5 μg/ml propidium iodide and analyzed by a BD FACSCalibur flow cytometer (BD Biosciences). DNA contents were analyzed using CellQuestPro software (BD Biosciences).

Affinity Purification and Immunoblotting—HeLa cells were lysed in a hypotonic lysis buffer (10 mM HEPES-KOH, pH 8.0, 1.5 mM $MgCl_2$, 10 mM KCl, 0.5 mM DTT, 0.5 mM PMSF) supplemented with phosphatase inhibitors (100 mM sodium orthovanadate, 5 mM $NaPP_i$, 60 mM glycerol 2-phosphate). Cells were lysed by Dounce homogenization, and proteins were extracted by addition of 1 volume of a whole cell extraction buffer (40 mM HEPES-KOH, pH 8.0, 1.5 mM $MgCl_2$, 0.4 mM EDTA, 50% glycerol, 1.2 M NaCl, 0.5 mM DTT) supplemented with a mixture of protease inhibitors (Sigma) and phosphatase inhibitors including 100 mM NaF. The lysates were centrifuged at 168,000 $\times$ *g* for 45 min at 4 °C. Supernatants were dialyzed overnight (20 mM HEPES-KOH, pH 8.0, 20% glycerol, 100 mM KCl, 0.2 mM EDTA, 0.5 mM PMSF, 0.5 mM DTT supplemented with phosphatase inhibitors). Dialyzed extracts (30 mg of total proteins/extract, equivalent to $5{\cdot}10^8$ asynchronous cells) were incubated for 5 h with M2 affinity resin pre-equilibrated in BC100 buffer (20 mM HEPES-KOH, pH 7.9, 20% glycerol, 100 mM KCl, 0.2 mM EDTA supplemented with phosphatase inhibitors). Resin was subsequently washed with 100 column volumes of BC300 buffer (40 mM Tris-HCl, pH 7.9, 20% glycerol, 300 mM KCl, 0.2 mM EDTA, 0.1% Nonidet P-40 supplemented with phosphatase inhibitors). Proteins were eluted with 1 column volume of BC300 buffer supplemented with 160 μg/ml FLAG peptide. The elution step was repeated once, and the fractions were pooled and subsequently incubated overnight with HA affinity resin pre-equilibrated in BC300 buffer. Resin was washed with BC300 buffer. Bait and interacting proteins were eluted at 30 °C with 2 mg/ml HA peptide. Recovery of the TBP bait was checked by immunoblotting using either anti-HA or anti-TBP antibody.

In-gel Tryptic Digestion—Protein eluates were separated on a gradient NuPAGE gel and visualized using Coomassie Blue staining. A gel lane was cut into slices, and each slice was cut into small (1-mm^3) pieces. The gel pieces were washed, in-gel reduced with dithiothreitol, alkylated with iodoacetamide, and digested overnight at 37 °C by adding trypsin at a concentration of 10 ng/ml as described by Wilm *et al.* (26).

On-line Nanoflow Liquid Chromatography FT-ICR-MS/MS—Peptides generated by in-gel digestion were analyzed by nanoflow liquid chromatography using an Agilent 1100 HPLC system (Agilent Technologies, Waldbronn, Germany) consisting of a solvent degasser, a binary pump, and a thermostated well-plate autosampler coupled on line to a 7-tesla linear trap quadrupole (LTQ)-FT mass spectrometer (Thermo Electron, Bremen, Germany). The system was operated in a setup essentially as described previously (27). Aqua C_{18} 5-μm resin (Phenomenex, Torrance, CA) was used for the trap column, and ReproSil-Pur C18-AQ 3-μm resin (Dr. Maisch GmbH, Ammerbuch, Germany) was used for the analytical column. Peptides were trapped at 5 μl/min in 100% solvent A (0.1 M acetic acid in water) on a 2-cm trap column (100-μm internal diameter, packed in house) and eluted to a 20-cm analytical column (50-μm internal diameter, packed in

Downloaded from http://www.mcponline.org/ by guest on October 20, 2019

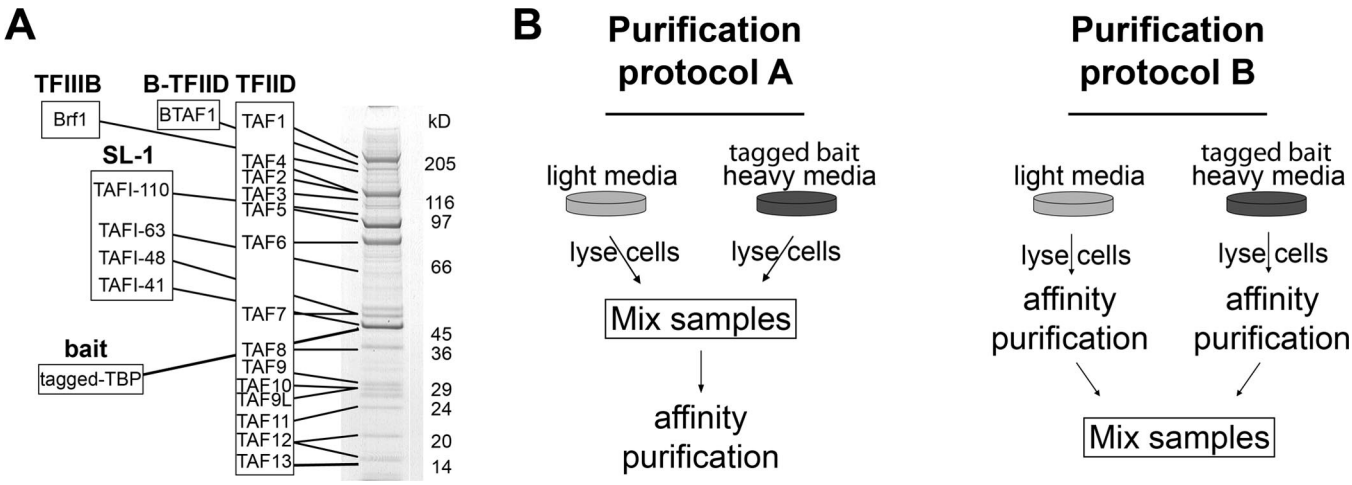

FIG. 1. **Experimental setup for the determination of dynamics within TBP complexes.** *A*, Coomassie-stained 1D SDS-polyacrylamide gel of affinity-purified samples. HA-FLAG-TBP expressed in HeLa S3 cells was affinity-purified, and the eluted proteins were separated by SDS-PAGE. Indicated on the *left side* of the gel are the identified proteins belonging to the different TBP-containing complexes, namely SL1, TFIID, B-TFIID, and TFIIIB. *B*, schematic representation of the two different affinity purification protocols used in this study. Control HeLa S3 cells were grown on light medium, whereas TBP HeLa S3 cells were grown on heavy medium. In a standard approach (purification protocol A, *left panel*), samples were mixed before the affinity purification step. To reveal specificity, a second sequence was used where samples were mixed after affinity purification (purification protocol B, *right panel*).

house) at about 150 nl/min in a 50-min gradient from 0 to 40% solvent B (0.1 M acetic acid in 8:2 (v/v) acetonitrile/water). The column eluent was sprayed directly into the ESI source of the mass spectrometer via a butt-connected nano-ESI emitter (New Objectives, Woburn, MA). The mass spectrometer was operated in data-dependent mode, automatically switching between MS and MS/MS acquisition. Full scan MS spectra (from *m/z* 300 to 1500) were acquired in FT-ICR with a resolution of 100,000 at *m/z* 400 after accumulation to a target value of 1,000,000. The two most intense ions at a threshold above 5000 were selected for collision-induced fragmentation in the linear ion trap at a normalized collision energy of 35% after accumulation to a target value of 10,000.

Protein Identification—In a postanalysis process, raw data were converted to peak lists using BioworksBrowser software, Version 3.1. For protein identification, MS/MS data were submitted to the International Protein Index (IPI) human (release 3.25, 67,250 sequence entries) using Mascot Version 2.1 (Matrix Science) with the following settings: 20 ppm and 0.8-Da deviation for precursor and fragment masses, respectively. Trypsin was specified as the proteolytic enzyme, and up to two missed cleavages were allowed. Carbamidomethylcysteine was set as fixed modification, and oxidized methionines, [$^{13}C_6$,$^{15}N_2$]lysine, and [$^{13}C_6$,$^{15}N_4$]arginine were set as variable modifications. Cutoffs of Mascot scores of peptides and proteins were set to 40 and 80, respectively, for considering them as being accurate identifications.

Protein Quantification—Relative quantification ratios of identified proteins were derived by MSQuant, which is open source software (SourceForge). Briefly peptide ratios between the monoisotopic peaks of light and heavy forms of the peptide were calculated and averaged over consecutive MS cycles for the duration of their respective LC-MS peaks in the total ion chromatogram using FT survey. Peptide ratios of the same protein were averaged to give protein abundance ratios as well as the respective standard deviation. Peptide ratios obtained by using the MSQuant software were all inspected manually.

Argine to proline conversion can be a potential limitation in SILAC experiments (28) but was only minor in the present experiments. In our data, the conversion of arginine to proline was estimated as 12%. In the mass spectra, this is seen as the formation of distinct peak clusters for all proline-containing peptides in the labeled state. This effect is even more pronounced if a peptide contains more than 1 proline residue. For a correct quantification these satellite peaks should be added to the peak intensity of the labeled peptides. The correct amount of the heavy state is therefore the sum of the Arg- and/or Lys-labeled peptide and the labeled peptide + [$^{13}C_5$,^{15}N]Pro peaks. These extra peaks should be added up to the labeled peptides to correct for the conversion. We corrected the quantification data for [$^{13}C_6$,$^{15}N_4$]arginine to [$^{13}C_5$,^{15}N]proline conversion for all peptides containing one or more proline residues using an in-house written script.

RESULTS AND DISCUSSION

We generated HeLa S3 cells expressing TBP tagged by the HA and FLAG epitopes at near endogenous levels (TBP HeLa S3 cells) (supplemental Fig. S1). The tagged TBP was efficiently incorporated into endogenous TBP complexes (supplemental Fig. S2). An extract of the TBP HeLa S3 cells was purified using anti-FLAG and anti-HA affinity resins. The sample was separated on a 1D gel, digested in gel with trypsin, and analyzed by mass spectrometry (Raw data, available as a Scaffold file, are available upon request.). Among the identified TBP-interacting proteins were all subunits of known TBP complexes, including the newly reported TAF_I41 subunit of SL1 (14) (Fig. 1*A*). The only exception to this was the Bdp1 subunit of TFIIIB that is known to dissociate easily (29). This confirmed the specificity of the TBP interactions and validated our approach for further characterization of TBP complexes expressed at endogenous levels in human cells. TAFs were not the only proteins to be identified in this experiment. Strikingly most of these other proteins were presented by low Mascot scores suggesting that they were substoichiometric to the TBP complexes. They included several subunits of the

Downloaded from http://www.mcponline.org/ by guest on October 20, 2019

TABLE I

SILAC ratios of TAFs identified after affinity purification of asynchronous extracts

Control and TBP HeLa S3 cells were grown in light and heavy media, respectively. SILAC ratios calculated in the experiment where samples were mixed before affinity purification are indicated in the protocol A column, whereas ratios calculated in the experiment where samples were mixed after affinity purification are indicated in the protocol B column. SILAC ratios were averaged over all quantified unique peptide pairs. Standard deviations are given. Peptide pair quant., number of unique peptide pairs used for the calculation of the ratios; ND, not determined.

Protein	IPI number	Purification protocol A			Purification protocol B		
		Peptide pair quant.	Ratio	S.D.	Peptide pair quant.	Ratio	S.D.
TBP	IPI00022831	3	0.01	0.01	3	0.00	0.00
BTAF1	IPI00024802	21	0.40	0.07	3	0.01	0.01
TAF1	IPI00009891	13	0.02	0.04	7	0.01	0.03
TAF2	IPI00328144	4	0.00	0.00	ND	ND	ND
TAF3	IPI00477959	4	0.00	0.00	ND	ND	ND
TAF4	IPI00413755	11	0.01	0.01	6	0.00	0.00
TAF4b	IPI00023258	2	0.00	0.00	ND	ND	ND
TAF5	IPI00298925	9	0.02	0.03	5	0.01	0.01
TAF6	IPI00028579	16	0.01	0.01	4	0.00	0.00
TAF7	IPI00018111	8	0.01	0.01	ND	ND	ND
TAF8	IPI00065313	ND	ND	ND	4	0.00	0.00
TAF9	IPI00002993	5	0.01	0.01	6	0.01	0.00
TAF9L	IPI00642105	2	0.00	0.00	2	0.00	0.00
TAF10	IPI00030364	2	0.01	0.00	2	0.00	0.00
TAF12	IPI00002806	5	0.01	0.01	4	0.01	0.01
TAF13	IPI00018108	3	0.01	0.00	2	0.01	0.01
TAF_I110	IPI00246842	7	0.00	0.01	5	0.00	0.01
TAF_I63	IPI00291416	3	0.00	0.00	2	0.00	0.00
TAF_I48	IPI00024263	2	0.01	0.01	ND	ND	ND
TAF_I40	IPI00012225	2	0.00	0.00	ND	ND	ND
Brf1	IPI00016859	6	0.10	0.06	2	0.00	0.00

SWI/SNF complexes (30) and the TFIIA subunits TFIIAα/β and TFIIAγ indicative of the TAC complex (31).

We next used SILAC to better distinguish between background proteins and TBP-binding proteins. For this purpose TBP HeLa S3 cells were grown in medium containing heavy ^{13}C,^{15}N-labeled arginine (Δmass = 10 Da) and ^{13}C,^{15}N-labeled lysine (Δmass = 8 Da), whereas control non-tagged HeLa S3 cells were grown in medium containing light versions of arginine and lysine. Mass spectrometric analysis showed that after six cell generations the labeled amino acids were fully incorporated (>98%) (data not shown). As described in the standard protocols (3, 7) cellular extracts were mixed in a ratio of 1:1 (total protein amount) before the affinity purification (Fig. 1*B*, *left panel*, purification protocol A). Samples were then processed for 1D gel separation and in-gel digestion with trypsin and analyzed by mass spectrometry. For all detected unique TAF peptides the ratio of the signal of their unlabeled version *versus* their labeled version (SILAC ratio) was determined (A list of all quantified peptides and proteins, including Mascot score, protein name, and IPI accession number, and raw data are available upon request). Then ratios were averaged over all quantified unique peptides corresponding to the same TAF (Table I, protocol A). Using this, we expected that TBP and proteins that specifically interact with TBP would be represented exclusively by isotope-labeled peptides, whereas nonspecific background proteins would yield both unlabeled and labeled peptides theoretically with equal intensities. Indeed for TBP, TFIID-TAFs, and also for all SL1 and TFIIIB subunits only labeled peptides could be detected in the mass spectra (Fig. 2, *A–C*, *left panels*, and Table I). In general, the SILAC ratios for those proteins ranged from 0.00 to 0.1 (Table I). Surprisingly and in contrast with the other TAFs, significant amounts of unlabeled peptides could be detected for BTAF1 (Fig. 2*D*, *left panel*, and Table I). The signal from the unlabeled peptides averaged over all detected peptides was ~40 ± 7% of the intensity of the labeled peptides. This result was highly reproducible as indicated by the average SILAC ratio of 0.37 ± 0.05 from three biologically independent experiments. In contrast, a background protein like tubulin β-2c displayed a SILAC ratio of ~1 (Fig. 2*E*, *left panel*).

We hypothesized that exchange of BTAF1 took place during the affinity purification process whereby BTAF1 from the unlabeled cell extracts exchanged to replace the labeled BTAF1 from extracts containing tagged TBP. To test this and to exclude that BTAF1 is a nonspecific TBP-interacting protein, the protocol of the affinity purification was changed. TBP HeLa S3 cells were grown in heavy medium, whereas control HeLa S3 cells were grown in light medium. Cellular extracts (same amount of total proteins) were separately affinity-purified, and only after this step eluted materials were mixed prior to 1D gel separation (Fig. 1*B*, *right panel*, purification protocol B). Again SILAC ratios were determined for all the TAFs (Table I, protocol B) (Raw data are available upon request.). As expected, in this experiment only labeled TAF peptides including BTAF1 peptides could be detected in the mass spectra (Fig. 2, *A–D*, *right panels*, and Table I). As a control, tubulin

Downloaded from http://www.mcponline.org/ by guest on October 20, 2019

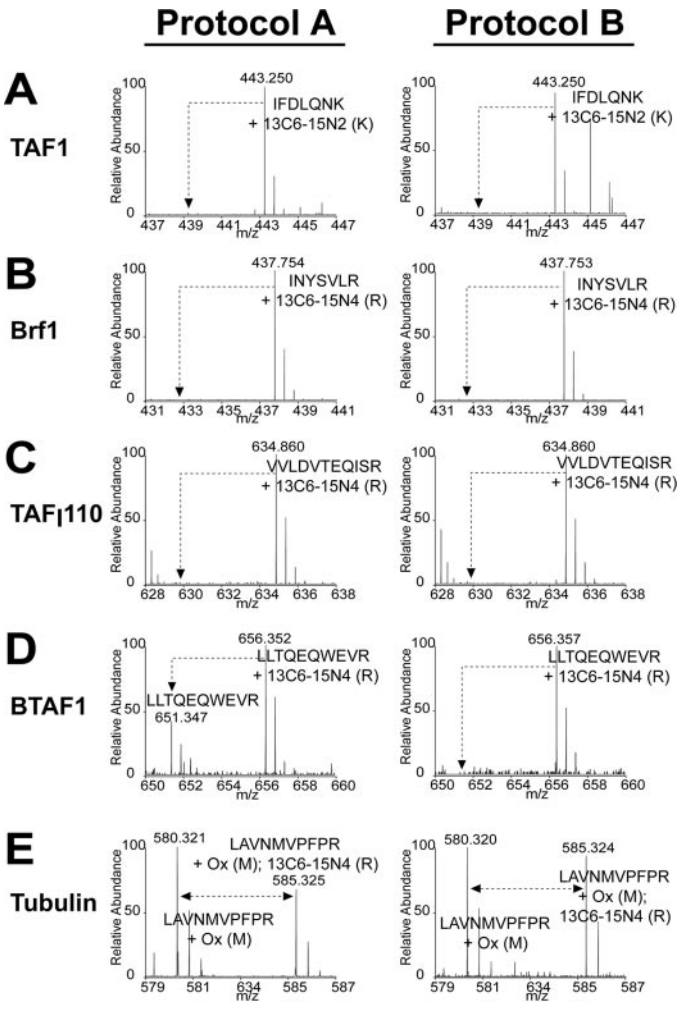

FIG. 2. **Representative peptide mass spectra of four different proteins belonging to distinct TBP complexes.** *A*, from the TFIID protein complex, the peptide IFDLQNK from TAF1 is shown. *B*, the peptide INYSVLR from BRF1 from the TFIIIB complex is depicted. *C*, VVLDVTEQISR from TAF_I110 from the SL1 complex is shown. *D*, LLTQEQWEVR from the protein BTAF1 from the B-TFIID complex. *E*, for comparison we included the spectra of a peptide of a nonspecific interacting protein, LAVNMVPFPR from tubulin β-2c. The mass spectra on the *left side* correspond to the experiment in which the samples from different cultures were mixed before affinity purification (protocol A), whereas the mass spectra on the *right side* originate from the experiment in which the samples were mixed after they have been affinity-purified (protocol B). It is indicated in the spectra if the labeled or unlabeled version of the peptide is present. If the unlabeled peptide is not present, an *arrow* indicates the position in the mass spectrum where it theoretically is expected.

β-2c-derived peptides again appeared with a SILAC ratio of about 1 (Fig. 2*E*, *right panel*). Together these results indicate that, complexed to TBP, BTAF1 is a dynamic protein. It is unlikely that this stems from a low affinity interaction as a K_d of 1 nM has been determined for the yeast orthologues (32). Besides it is unlikely that the abundant amount of unlabeled BTAF1 peptides is a consequence of oligomerization of the protein. BTAF1 coelutes with TBP from gel filtration columns in fractions corresponding to a 300-kDa complex and is not present in any higher molecular mass complexes (Refs. 33 and 34 and supplemental Fig. S2). It is also important to note that the dynamic behavior of BTAF1 was not shared by any of the other TAFs of the TFIID, SL1, and TFIIIB complexes under our experimental conditions. The results indicate that in combining SILAC and affinity purification the sequence of the different steps is crucial in determining the specificity of the interactions and can reveal subunit exchange between protein complexes.

In a new step we investigated whether the affinity purification protocol A could be applied to study the exchange of recombinant proteins within complexes. To this end, light baculovirus-expressed BTAF1 protein (supplemental Fig. S3) was added to the isotope-labeled TBP HeLa S3 or control HeLa S3 cell extracts. These mixtures were then purified using the protocol A (Fig. 1*B*, *left panel*). Significant amounts of unlabeled BTAF1 peptides were detected only if recombinant BTAF1 had been added to the tagged TBP HeLa S3 cell extract (Fig. 3, *A* and *B*). Increasing the amount of BTAF1 added to the cell extract resulted in increased amounts of unlabeled BTAF1 peptides, and the use of light recombinant B-TFIID complex also led to the detection of unlabeled BTAF1 peptides (data not shown). Together these results indicate that recombinant BTAF1 is dynamic at the expense of the endogenous BTAF1 protein and is able to exchange between TBP complexes. Furthermore it validates the use of recombinant proteins to investigate dynamics within complexes. Our proteomics approach was confirmed by TBP co-immunoprecipitation experiments mixing purified recombinant His-tagged BTAF1 with recombinant B-TFIID (non-tagged BTAF1/His-tagged TBP). Fig. 4*A* shows that His-tagged BTAF1 is co-immunoprecipitated with TBP already engaged in a B-TFIID complex. This result validates the exchange of BTAF1 subunit within the B-TFIID complex and indicated that this is an intrinsic property of the complex.

Next we investigated the dynamic behavior of different TBP complexes during the cell cycle as several reports indicate regulation of TBP complexes during mitosis (22). Whole cell extracts were prepared from cells treated with nocodazole for 17 h. Fluorescence-activated cell sorter analysis of propidium iodide-stained cells indicated that 85 $\pm$ 4% of the cells were arrested in mitosis (supplemental Fig. S4). Using the mitotic cell extracts the observed signals of the unlabeled BTAF1 peptides represented only 0.02 $\pm$ 0.01 of the labeled peptides when samples were mixed before the affinity purification (protocol A) compared with 0.40 $\pm$ 0.07 in the asynchronous cells (Fig. 3, *A* and *C*) (Raw data are available upon request.). The average SILAC ratio of two biologically independent experiments was 0.05 $\pm$ 0.03 showing that results obtained with mitotic extracts are highly reproducible. The lack of detection of unlabeled BTAF1 peptide did not stem from a difference in relative amount of BTAF1 *versus* TBP in mitotic extract compared with asynchronous extract (supplemental Fig. S1). Again when the samples were mixed after the purification

Downloaded from http://www.mcponline.org/ by guest on October 20, 2019

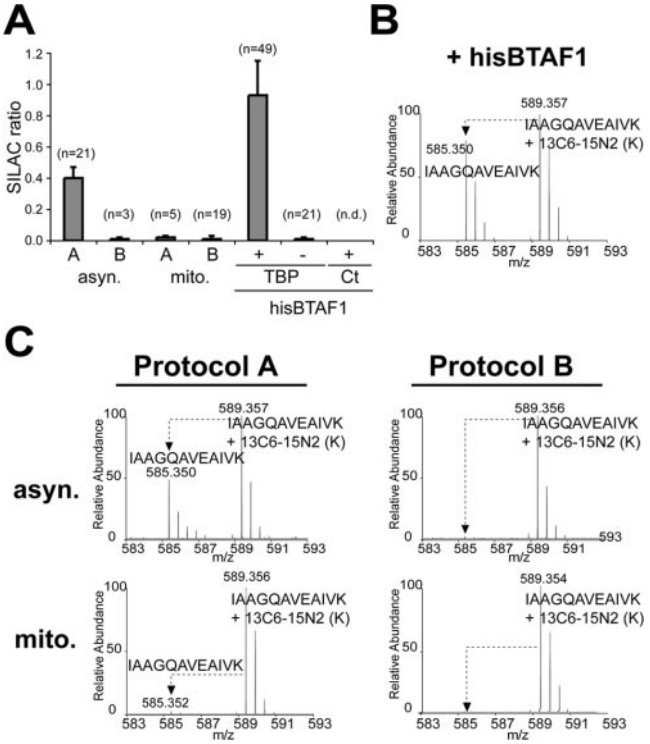

FIG. 3. **Dynamics of B-TFIID is a regulated process.** *A*, SILAC ratios of BTAF1 peptides have been determined in three different experimental setups. In a first experiment, control and TBP HeLa S3 cells were grown in light and heavy media, respectively. Samples were combined according to purification protocol A or B. In a second experiment, mitotic control and TBP HeLa S3 cells were grown in light and heavy media, respectively. Samples were combined according to purification protocol A or B. In a third experiment, 150 μg of unlabeled recombinant His-tagged BTAF1 were mixed either with TBP or control (*Ct*) HeLa S3 cell extracts, and samples were affinity-purified according to protocol A. As a control TBP HeLa S3 cell extract was purified without addition of recombinant BTAF1. All samples of the three experiments were further analyzed by mass spectrometry, and ratios of unlabeled *versus* labeled BTAF1 peptide signal were determined. The average ratio of unique peptide pairs used for quantification is given for one representative experiment. The number of unique peptide pairs used for quantification is given in *parentheses*. *n.d.*, not determined. *B*, representative IAAGQAVEAIVK BTAF1 peptide mass spectrum is shown for the experiment where recombinant His-tagged BTAF1 was mixed with TBP HeLa S3 extract prior to affinity purification. *C*, representative IAAGQAVEAIVK BTAF1 peptide mass spectra are shown for the experiments using mitotic extracts (*lower panels*). For comparison, mass spectra of the same peptide obtained for experiments using asynchronous extracts are included (*upper panels*). The mass spectra on the *left side* correspond to the experiment in which the samples from different cultures were mixed before affinity purification (protocol A), whereas the mass spectra on the *right side* originate from the experiment in which the samples were mixed after they have been affinity-purified (protocol B). It is indicated in the spectra if the labeled or unlabeled version of the peptide is present. If the unlabeled peptide is not present, an *arrow* indicates the position in the mass spectrum where it theoretically is expected. *mito*., mitotic; *asyn*., asynchronous.

steps (protocol B), no unlabeled BTAF1 peptides could be detected (Fig. 3, *A* and *C*). This indicates that BTAF1 exchange is significantly inhibited in mitotic cell extracts. Similar

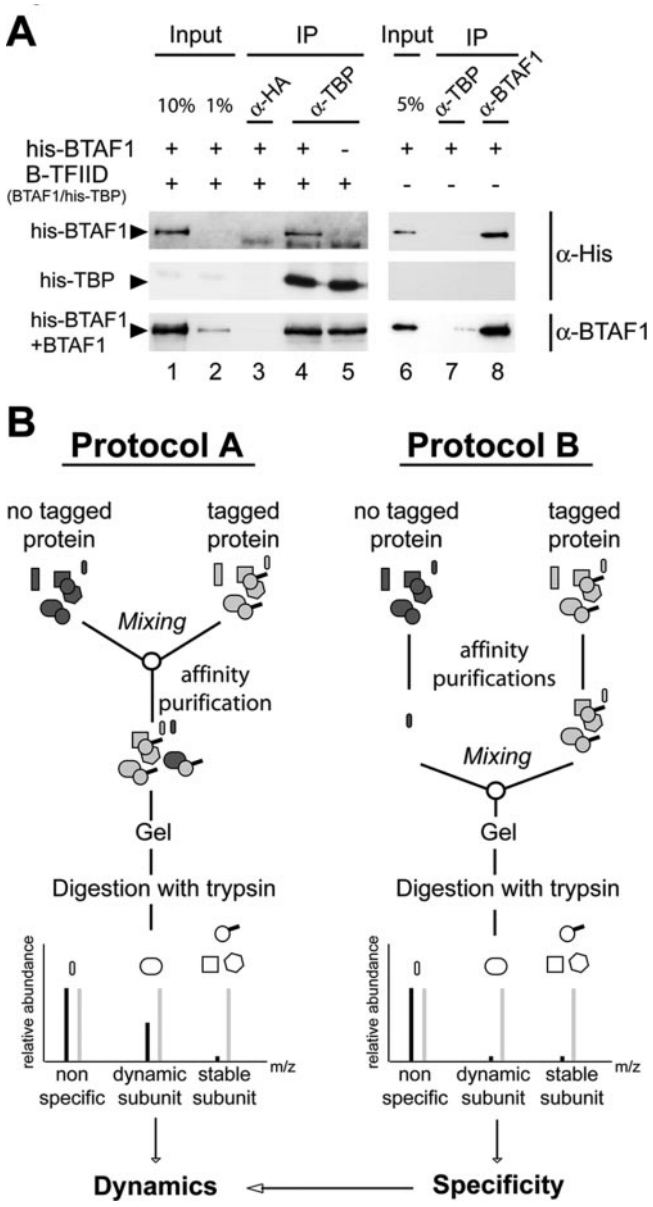

FIG. 4. **Evaluation of subunit exchange by quantitative mass spectrometry.** *A*, purified recombinant B-TFIID (non-tagged BTAF1/His-tagged TBP) was incubated with (*lanes 3* and *4*) or without (*lane 5*) purified recombinant His-tagged BTAF1. Immunoprecipitation (*IP*) was performed as indicated with anti-TBP (1F8) (*lanes 4* and *5*) or anti-HA (12CA5) (*lane 3*), and bound proteins were analyzed by immunoblotting with anti-BTAF1 and anti-His as indicated. 10 and 1% inputs are indicated in *lanes 1* and *2*. As a control His-tagged BTAF1 alone was immunoprecipitated with anti-TBP (1F8) (*lane 7*) or anti-BTAF1 (Pf299) (*lane 8*). *B*, specificity and dynamics are revealed by the combination of two different protocols in SILAC/affinity purification. A control cell line is grown in light medium, whereas a tagged bait cell line is grown in heavy medium. Extracts are mixed before the affinity purification step in protocol A, whereas extracts are separately affinity-purified, and eluted materials are mixed prior to 1D gel separation in protocol B. Using the protocol B to mix the samples (after affinity purification) assigns specific and nonspecific interactions with the bait, whereas using the protocol A to mix the samples (before affinity purification) reveals dynamic and stable subunits by comparison with the protocol B data.

Downloaded from http://www.mcponline.org/ by guest on October 20, 2019

to extracts from asynchronous cells, no unlabeled peptides from the other TAFs could be detected in the mitotic samples either after protocol A or B of affinity purification (the determined SILAC ratios were lower than 0.04 with Brf1 having the highest value), indicating that the other TAFs do not exchange during mitosis (supplemental Table 2).

To summarize, the combination of different purification protocols allows investigation of both specificity and dynamics of protein interactions involving TBP. We found that the BTAF1 subunit of B-TFIID displays dynamic properties and that TFIID, SL1, and TFIIIB represent relatively stable complexes in cell extracts. This dynamic behavior of BTAF1 is inhibited in mitotic cell extracts. It is tempting to speculate about the functional consequences and the mechanism of mitotic inhibition of BTAF1 exchange. In human cells, a large proportion of TBP is associated with BTAF1 indicating that the protein is an important regulator of TBP function (16). Current models for BTAF1 function involve delivery of TBP to promoter sites and/or releasing this protein from (non-promoter) DNA to facilitate (re)distribution of TBP. The lack of exchange within the soluble B-TFIID complex during mitosis, a phase where transcription is drastically inhibited, would constitute a mechanism to prevent deposition of TBP onto DNA. In fact, TBP has been shown to be excluded from condensed mitotic chromatin (22, 35). Several mechanisms can account for the observed inhibition, which could involve the action of mitotic kinases, negative cofactors (36), or sumoylation pathways (37). The results presented here provide a basis for further experiments addressing these possibilities.

Our observations provide a new and generic application of affinity purification in combination with SILAC to identify and investigate the dynamic subunits of protein complexes. These components can be revealed by comparing results of the two protocols in SILAC/affinity purification (Fig. 4*B*). This SILAC-based proteomics strategy is widely applicable to investigate and to quantify the dynamic properties of individual subunits in large multiprotein complexes. It offers the possibility to examine effects of (mutated forms of) recombinant subunits or subassemblies. Complexes can be isolated from cells under different physiological conditions, during different stages of differentiation or cell cycle (as here), or treated with various growth stimuli or inhibitors. Our methodology also allows testing of (small molecule) regulators on complex/subunit exchange. As such this quantitative proteomics strategy adds a new dimension to the study of regulation and dynamics of protein-protein interactions.

Acknowledgments—We gratefully acknowledge Drs. Rene Medema and Geert Kops for advice on preparing mitotic cells. We thank Marcel Winter for help with the bioreactor. We thank Koen Dreijerink, Guillaume Lenoir, Klaas Mulder, and Folkert van Werven for critical reading of the manuscript. We thank Joost Gouw and Bas van Breukelen for adapting MSQuant for our analyses and for bioinformatics assistance. We also thank members of the Timmers and Heck laboratories for stimulating discussions.

* This work was supported in part by grants from the European Union (Grant STREP LSHG-CT-2004–502950) (to the Timmers laboratory) and the Netherlands Proteomics Centre. The costs of publication of this article were defrayed in part by the payment of page charges. This article must therefore be hereby marked "*advertisement*" in accordance with 18 U.S.C. Section 1734 solely to indicate this fact.

S The on-line version of this article (available at http://www.mcponline.org) contains supplemental material.

§ Both authors contributed equally to this work.

¶ Supported by Human Frontier Science Program Grant LT-0860/2005 and Fondation Recherche Médicale Grant SPE20031212256.

** Present address: National Inst. of Public Health and Environment (RIVM), P. O. Box 1, 3720 Bilthoven, The Netherlands.

‡‡ These authors contributed equally to this work.

§§ To whom correspondence may be addressed: Dept. of Physiological Chemistry, University Medical Centre Utrecht, Universiteitsweg 100, P. O. box 85060, 3508 AB Utrecht, The Netherlands. E-mail: h.t.m.timmers@umcutrecht.nl.

¶¶ To whom correspondence may be addressed: Biomolecular Mass Spectrometry and Proteomics, Bijvoet Center for Biomolecular Research and Utrecht Institute for Pharmaceutical Sciences, Utrecht University, Sorbonnelaan 16, 3584 CA Utrecht, The Netherlands. E-mail: a.j.r.heck@uu.nl.

REFERENCES

1. Romijn, E. P., Christis, C., Wieffer, M., Gouw, J. W., Fullaondo, A., van der Sluijs, P., Braakman, I., and Heck, A. J. (2005) Expression clustering reveals detailed co-expression patterns of functionally related proteins during B cell differentiation: a proteomic study using a combination of one-dimensional gel electrophoresis, LC-MS/MS, and stable isotope labeling by amino acids in cell culture (SILAC). *Mol. Cell. Proteomics* **4,** 1297–1310
2. Everley, P. A., Krijgsveld, J., Zetter, B. R., and Gygi, S. P. (2004) Quantitative cancer proteomics: stable isotope labeling with amino acids in cell culture (SILAC) as a tool for prostate cancer research. *Mol. Cell. Proteomics* **3,** 729–735
3. Blagoev, B., Kratchmarova, I., Ong, S. E., Nielsen, M., Foster, L. J., and Mann, M. (2003) A proteomics strategy to elucidate functional protein-protein interactions applied to EGF signaling. *Nat. Biotechnol.* **21,** 315–318
4. Ong, S. E., Blagoev, B., Kratchmarova, I., Kristensen, D. B., Steen, H., Pandey, A., and Mann, M. (2002) Stable isotope labeling by amino acids in cell culture, SILAC, as a simple and accurate approach to expression proteomics. *Mol. Cell. Proteomics* **1,** 376–386
5. Schulze, W. X., and Mann, M. (2004) A novel proteomic screen for peptide-protein interactions. *J. Biol. Chem.* **279,** 10756–10764
6. Ranish, J. A., Yi, E. C., Leslie, D. M., Purvine, S. O., Goodlett, D. R., Eng, J., and Aebersold, R. (2003) The study of macromolecular complexes by quantitative proteomics. *Nat. Genet.* **33,** 349–355
7. Trinkle-Mulcahy, L., Andersen, J., Lam, Y. W., Moorhead, G., Mann, M., and Lamond, A. I. (2006) Repo-Man recruits PP1γ to chromatin and is essential for cell viability. *J. Cell Biol.* **172,** 679–692
8. Tackett, A. J., DeGrasse, J. A., Sekedat, M. D., Oeffinger, M., Rout, M. P., and Chait, B. T. (2005) I-DIRT, a general method for distinguishing between specific and nonspecific protein interactions. *J. Proteome Res.* **4,** 1752–1756
9. Shiio, Y., and Aebersold, R. (2006) Quantitative proteome analysis using isotope-coded affinity tags and mass spectrometry. *Nat. Protoc.* **1,** 139–145
10. Alberts, B. (1998) The cell as a collection of protein machines: preparing the next generation of molecular biologists. *Cell* **92,** 291–294
11. Sharp, P. A. (1992) TATA-binding protein is a classless factor. *Cell* **68,** 819–821
12. Timmers, H. T., and Sharp, P. A. (1991) The mammalian TFIID protein is present in two functionally distinct complexes. *Genes Dev.* **5,** 1946–1956
13. Tora, L. (2002) A unified nomenclature for TATA box binding protein (TBP)-associated factors (TAFs) involved in RNA polymerase II transcription. *Genes Dev.* **16,** 673–675

Downloaded from http://www.mcponline.org/ by guest on October 20, 2019

14. Gorski, J. J., Pathak, S., Panov, K., Kasciukovic, T., Panova, T., Russell, J., and Zomerdijk, J. C. (2007) A novel TBP-associated factor of SL1 functions in RNA polymerase I transcription. *EMBO J.* **26,** 1560–1568
15. Geiduschek, E. P., and Kassavetis, G. A. (2001) The RNA polymerase III transcription apparatus. *J. Mol. Biol.* **310,** 1–26
16. Pereira, L. A., Klejman, M. P., and Timmers, H. T. (2003) Roles for BTAF1 and Mot1p in dynamics of TATA-binding protein and regulation of RNA polymerase II transcription. *Gene* (*Amst*.) **315,** 1–13
17. Pugh, B. F. (2000) Control of gene expression through regulation of the TATA-binding protein. *Gene* (*Amst*.) **255,** 1–14
18. Mengus, G., Fadloun, A., Kobi, D., Thibault, C., Perletti, L., Michel, I., and Davidson, I. (2005) TAF4 inactivation in embryonic fibroblasts activates TGFβ signalling and autocrine growth. *EMBO J.* **24,** 2753–2767
19. Bell, B., Scheer, E., and Tora, L. (2001) Identification of hTAF(II)80δ links apoptotic signaling pathways to transcription factor TFIID function. *Mol. Cell* **8,** 591–600
20. Gegonne, A., Weissman, J. D., Zhou, M., Brady, J. N., and Singer, D. S. (2006) TAF7: a possible transcription initiation check-point regulator. *Proc. Natl. Acad. Sci. U. S. A.* **103,** 602–607
21. Prescott, D. M., and Bender, M. A. (1962) Synthesis of RNA and protein during mitosis in mammalian tissue culture cells. *Exp. Cell Res.* **26,** 260–268
22. Segil, N., Guermah, M., Hoffmann, A., Roeder, R. G., and Heintz, N. (1996) Mitotic regulation of TFIID: inhibition of activator-dependent transcription and changes in subcellular localization. *Genes Dev.* **10,** 2389–2400
23. Hu, P., Wu, S., and Hernandez, N. (2003) A minimal RNA polymerase III transcription system from human cells reveals positive and negative regulatory roles for CK2. *Mol. Cell* **12,** 699–709
24. Fairley, J. A., Scott, P. H., and White, R. J. (2003) TFIIIB is phosphorylated, disrupted and selectively released from tRNA promoters during mitosis in vivo. *EMBO J.* **22,** 5841–5850
25. Pereira, L. A., Klejman, M. P., Ruhlmann, C., Kavelaars, F., Oulad-Abdelghani, M., Timmers, H. T., and Schultz, P. (2004) Molecular architecture of the basal transcription factor B-TFIID. *J. Biol. Chem.* **279,** 21802–21807
26. Wilm, M., Shevchenko, A., Houthaeve, T., Breit, S., Schweigerer, L., Fotsis, T., and Mann, M. (1996) Femtomole sequencing of proteins from polyacrylamide gels by nano-electrospray mass spectrometry. *Nature* **379,** 466–469
27. Meiring, H. D., van der Heeft, E., ten Hove, G. J., and de Jong, A. P. J. M. (2002) Nanoscale LC-MS$^{(n)}$: technical design and applications to peptide and protein analysis. *J. Sep. Sci.* **25,** 557–568
28. Van Hoof, D., Pinkse, M. W., Oostwaard, D. W., Mummery, C. L., Heck, A. J., and Krijgsveld, J. (2007) An experimental correction for arginine-to-proline conversion artifacts in SILAC-based quantitative proteomics. *Nat. Methods* **4,** 677–678
29. Lobo, S. M., Tanaka, M., Sullivan, M. L., and Hernandez, N. (1992) A TBP complex essential for transcription from TATA-less but not TATA-containing RNA polymerase III promoters is part of the TFIIIB fraction. *Cell* **71,** 1029–1040
30. Wang, W., Cote, J., Xue, Y., Zhou, S., Khavari, P. A., Biggar, S. R., Muchardt, C., Kalpana, G. V., Goff, S. P., Yaniv, M., Workman, J. L., and Crabtree, G. R. (1996) Purification and biochemical heterogeneity of the mammalian SWI-SNF complex. *EMBO J.* **15,** 5370–5382
31. Mitsiou, D. J., and Stunnenberg, H. G. (2000) TAC, a TBP-sans-TAFs complex containing the unprocessed TFIIA$\alpha\beta$ precursor and the TFIIAγ subunit. *Mol. Cell* **6,** 527–537
32. Gumbs, O. H., Campbell, A. M., and Weil, P. A. (2003) High-affinity DNA binding by a Mot1p-TBP complex: implications for TAF-independent transcription. *EMBO J.* **22,** 3131–3141
33. Timmers, H. T., Meyers, R. E., and Sharp, P. A. (1992) Composition of transcription factor B-TFIID. *Proc. Natl. Acad. Sci. U. S. A.* **89,** 8140–8144
34. van der Knaap, J. A., Borst, J. W., van der Vliet, P. C., Gentz, R., and Timmers, H. T. (1997) Cloning of the cDNA for the TATA-binding protein-associated factorII170 subunit of transcription factor B-TFIID reveals homology to global transcription regulators in yeast and Drosophila. *Proc. Natl. Acad. Sci. U. S. A.* **94,** 11827–11832
35. Kieffer-Kwon, P., Martianov, I., and Davidson, I. (2004) Cell-specific nucleolar localization of TBP-related factor 2. *Mol. Biol. Cell* **15,** 4356–4368
36. Klejman, M. P., Pereira, L. A., van Zeeburg, H. J., Gilfillan, S., Meisterernst, M., and Timmers, H. T. (2004) NC2α interacts with BTAF1 and stimulates its ATP-dependent association with TATA-binding protein. *Mol. Cell. Biol.* **24,** 10072–10082
37. Wang, Z., Jones, G. M., and Prelich, G. (2006) Genetic analysis connects SLX5 and SLX8 to the SUMO pathway in Saccharomyces cerevisiae. *Genetics* **172,** 1499–1509

Downloaded from http://www.mcponline.org/ by guest on October 20, 2019